Check for updates

CSE/H₂S ameliorates colitis in mice *via* protection of enteric glial cells and inhibition of the RhoA/ROCK pathway

Song Wang[1], Yanyu Ding[2] and Wenjun Jiang[1]*

[1]Department of Gastroenterology, The First Affiliated Hospital of USTC, Division of Life Sciences and Medicine, University of Science and Technology of China, Hefei, China, [2]Department of Pharmacology, School of Basic Medical Sciences, Anhui Medical University, Hefei, China

The enteric glial cells (EGCs) participate in the homeostasis of the gastrointestinal tract, and RhoA/ROCK signaling pathway plays a vital role in colonic tight junctions. Hydrogen sulfide (H₂S) has been reported to alleviate colitis. However, the effect and mechanism of endogenous H₂S on colitis remain unclear. This study established a Cystathionine-γ-lyase (CSE) knockout mouse model, a significant source of H₂S production in the gut. The role of CSE-produced H₂S on EGCs and the RhoA/ROCK signaling pathway was investigated in experimental colitis using CSE knockout (KO) and wild-type (WT) mice. CSE gene knockout animals presented with disease progression, more deteriorated clinical scores, colon shortening, and histological damage. EGCs dysfunction, characterized by decreased expression of the glial fibrillary acidic protein (GFAP), C3, and S100A10, was observed in the colon of WT and KO mice, especially in KO mice. RhoA/ROCK pathway was significantly upregulated in colon of colitis mice, which was more evident in KO mice. Pretreatment with NaHS, an exogenous H₂S donor, significantly ameliorated mucosal injury and inhibited the expression of proinflammatory factors. Furthermore, we found that NaHS promoted the transformation of EGCs from "A1" to "A2" type, with decreased expression of C3 and increased expression of S100A10. These findings suggest that CSE/H₂S protects mice from colon inflammation, which may be associated with preserving EGCs function by promoting EGCs transformation and inhibiting the RhoA/ROCK pathway.

Introduction

Inflammatory bowel diseases (IBDs) are chronic progressive and unpredictable inflammatory diseases of gastroenteric tissue, which primarily include Crohn's disease and ulcerative colitis (UC) (1). Between 1990 and 2017, China experienced an increase in the age-standardized rate of prevalence, incidence, and the years of life lived with disability of IBD (2). The clinical manifestations of UC include diarrhea, abdominal pain, weight loss, and bloody stools, where sustained remission is not currently achievable (3). Although there have been many studies on UC, its pathological mechanism remains poorly understood. Previous immunological and genetic studies have demonstrated that the inflammation in UC patients was closely associated with a burst of cytokines or/and chemokines production from immune cells and epithelial cells, which was linked to the dysfunction of intestinal epithelial barrier (IEB) homeostasis (3, 4).

Enteric neurons and glial cells (EGCs) play a significant role in maintaining IEB function. However, enteric neurons alone couldn't maintain normal function, they are part of enteric nervous system and brain-gut axis, and EGCs are found accompanying enteric neurons throughout the gut (5). EGCs contribute to restoring the integrity of injured epithelium in IBD, and the ablation of EGCs leads to increased IEB permeability and intestinal inflammation (6, 7). EGCs present abnormalities in UC. EGCs dysfunction, manifested by the decrease of GFAP, was observed in dextran sodium sulfate (DSS)-induced murine UC (4). Neurotrophic growth factors can stabilize the intestinal barrier by preventing the apoptosis of EGCs and enterocytes (8).

Hydrogen sulfide (H_2S) is a ubiquitous second messenger molecule. H_2S is considered the third gasotransmitter, in addition to nitric oxide (NO) and carbon monoxide (CO). It is involved in inflammation, gut motility, oxidative stress, ulcer healing, vascular tone, neuromodulation, cryoprotection, memory formation, hormone secretion, apoptosis, and other vital biologic functions (9). H_2S in the gut is produced by the enzymes cystathionine-β-synthase (CBS) and Cystathionine-γ-lyase (CSE) of the host and sulfate-reducing bacteria (SRB) of intestinal resident microbes (9–11). CBS is the main source of H_2S in the central nervous system and CSE is the major source in the peripheral system (12). Grasa et al. found the interaction between TLR2 and TLR4 and the sulfide system in regulating colonic motility (11). However, detailed interactions of H_2S with other signaling mediator has not yet been elucidated. The RhoA/ROCK signaling pathway is related to UC (13). Inhibiting the RhoA/ROCK pathway might be a new approach in treating UC (14, 15). Moreover, we previously found that exogenous H_2S protects colon in murine UC by inhibiting the RhoA/ROCK pathway (16). CSE-derived H_2S inhibited reactive astrocyte proliferation and promoted functional neural recovery after cerebral ischemia/reperfusion injury in mice *via* the RhoA/

$ROCK_2$ pathway (17). However, the effect and mechanism of endogenous H_2S on the EGCs function and RhoA/ROCK signaling pathway following colitis are still unclear.

Considering the crucial role of EGCs function and RhoA/ROCK signaling pathway, as well as the potential therapeutic effect of H_2S in UC, this study was to investigate whether CSE-derived H_2S could alleviate DSS-induced acute intestinal inflammation by improving the recovery of EGCs dysfunction and inhibiting inflammation through targeted down-regulation of the RhoA/ROCK signaling pathway.

Materials and methods

Reagents

NaHS was purchased from Sigma Aldrich (St. Louis, USA); Dextran sulfate sodium (DSS, 36–50kDa) was purchased from Shanghai Yi Sheng Biological Company (Shanghai, China); Primary CSE, glial fibrillary acidic protein (GFAP), C3, S100 calcium-binding protein A10 (S100A10), RhoA, $ROCK_1$, and $ROCK_2$ antibodies were obtained from Abcam (San Francisco, CA, USA); Horseradish peroxidase-conjugated secondary antibodies were obtained from Santa Cruz Biotechnology (Santa Cruz, CA, USA). RhoA, $ROCK_1$, $ROCK_2$, Interleukin-6 (IL-6), H_2S, and tumor necrosis factor-α (TNF-α) test kits were obtained from Jiangsu Meimian Biological Company (Nanjing, China).

Experimental animals

Adult (6–8weeks) CSE knockout (KO) and wild-type (WT) C57BL/6 mice weighing 20 to 24g were supplied by Shanghai Bio model Organism Science & Technology Development Co., Ltd.; all animals were kept in-house, housed with a 12-h light/dark cycle per day and constant temperature (22 ± 2°C) and relative humidity (55 ± 5%). The mice were raised to adapt to the new environment for one week before the experiment. All animals have free access to a standard diet and water ad libitum. The program was approved by the Animal Experimental Ethics Review Committee of the University of Science and Technology of China under protocol number 2019-N(A)-196.

Experimental design and drug treatment

Thirty-six mice were randomly divided into six groups (n = 6). Two groups (WT control and KO control) received sterilized tap water ad libitum, and the other animals received 3% DSS dissolved in drinking water for seven days to induce colitis. Two groups (WT DSS+NaHS and KO DSS+NaHS) received NaHS at 4.8mg/kg by intraperitoneal injection, as previously reported (16, 17). On

the 7th day, all mice were sacrificed 12 h later after the last administration. The length of the colons was measured and then washed instantly using ice-cold physiological saline. One part of colon was rapidly divided and fixed in 10% formalin for pathological examination, and the remaining parts were stored at −80°C for western blotting assay and immunofluorescence.

Disease activity index

The severity of colitis was assessed by monitoring the disease activity index (DAI) during acute colitis, including body weight loss, stool consistency, and fecal bleeding. The DAI was calculated as described previously (18). The difference between the initial and testing weights was calculated as weight loss. Fecal bleeding was tested using a fecal occult blood test kit—two independent observers who were blinded to the experimental conditions accumulated the DAI scores.

Histological examination

The mouse colon sections were fixed in 4% phosphate-buffered saline (PBS)-buffered formalin for 48 h. Then, the samples were dehydrated, embedded in paraffin, and cut into 4-μm fractions. The sections were stained with hematoxylin and eosin (H&E) and observed under light microscopy. Histological scores were calculated by two pathologists uninformed of the experimental grouping. Each sample was graded semi-quantitatively from 0 to 3 based on four criteria: (1) leucocyte infiltration in the lamina propria; (2) degree of epithelial hyperplasia and goblet cell depletion; (3) area of tissue affected; and (4) presence of markers of severe inflammation such as crypt abscesses, submucosal inflammation, and ulcers (19).

ELISA assays of inflammatory cytokine expression

After the behavior experiment, the mice were killed under deep anesthesia, and the sera were collected. The colon was cut into small pieces and homogenized with iced cold Tris-HCl buffer to extract total protein. The expression levels of cytokines IL-6 (Cat No.2101M08) and TNF-α(Cat No.2101M26) in the serum of mice and the RhoA(Cat No.2108M36), $ROCK_1$(Cat No.2108M24), $ROCK_2$(Cat No.2108M41), and H_2S(Cat No.2109M33) contents in the colon were measured by enzyme-linked immunosorbent assay (ELISA) kits (Jiangsu Meimian Biological Company). All procedures followed the manufacturer's guidelines. IL-6 and TNF-α were expressed as pg/ml, and the RhoA, $ROCK_1$, $ROCK_2$, and H_2S content was expressed as ng/ml, IU/L, IU/L, and nmol/g protein, respectively.

The intra-assay coefficient of variation (CV) and inter-assay CV were less than 10% and 15%, respectively.

Western blotting analysis

As described previously, the total protein was extracted from colon tissues after the mice were decapitated under deep anesthesia and quantified using a protein assay kit (Beyotime Biotechnology, Shanghai, China) (16). Equal amounts of proteins were loaded and separated by electrophoresis and then transferred onto polyvinylidene difluoride membranes. The membranes were blocked with 5% defatted milk in Tris-buffered saline with 0.05% Tween 20 for one h at room temperature and then incubated with primary antibodies against RhoA, $ROCK_1$, $ROCK_2$, GFAP, S100A10, C3, or GAPDH overnight at 4°C. The catalog numbers and dilutions of each antibody are shown in Table 1. After incubation with the corresponding secondary antibody (1: 5000) for one h at room temperature, the membranes were visualized with an ECL (enhanced chemiluminescence) kit (Thermo Fisher Scientific, Massachusetts, USA) and scanned with a Chemi Q4800 mini imaging system (Shanghai Bioshine Technology, Shanghai, China). The relative expression levels of proteins were corrected by GAPDH.

Immunofluorescence

Paraffin-embedded colon sections were deparaffinized in xylene and rehydrated through graded alcohol to water. After unmasking antigens by 0.01 mol/L citrate buffer solution, the colon sections were blocked with 2% BSA and stained with anti-Myelin basic protein (MBP) (Santa Cruz, USA), anti-Neuronal Nuclei (NeuN)(Abcam), and anti-GFAP (Abcam), anti-C3 (Abcam), and anti-S100A10(Abcam) primary antibodies overnight at 4°C. Signals were determined using FITC-conjugated secondary antibodies (Boster Biological Technology) and then counterstained with 4',6-diamidino-2-phenylindole (DAPI) (Abcam). The catalog numbers and dilutions of each antibody are shown in Table 1. Images were collected on a Leica TCS SPS microscope (Wetzlar, Germany), for fluorescence microscopy was used for nuclear counterstaining. ImageJ software was used to analyze fluorescence intensity in colon sections statistically.

Statistical analysis

Data were analyzed using SPSS 25.0 (IBM, Armonk, NY, USA) software. GraphPad Prism 5.0 (GraphPad; San Diego, CA, USA) was used for statistical analysis. Results are shown as the mean ± S.E.M. The mean between groups was analyzed by

TABLE 1   Antibodies used in the study.

Antibody	Company	Order Number	WB	IF
Anti-GFAP	Affinity, China	GB12096	1:2000	1:200
Anti-S100a10	Abcam, USA	Ab76472	1:5000	1:100
Anti-C3	Abcam, USA	Ab200999	1:2000	1:100
Anti-RhoA	Abcam, USA	Ab187027	1:5000	
Anti-ROCK$_1$	Abcam, USA	Ab134181	1:5000	
Anti-ROCK$_2$	Abcam, USA	Ab125025	1:5000	
Anti-NeuN	Abcam, USA	Ab279296		1:100
Anti-MBP	Santa Cruz, USA	sc271524		1:100
Anti-GAPDH	Affinity, China	Ab-AF7021	1:5000	
Peroxidase-Conjugated Goat anti-Rabbit IgG(H+L)	Zhongshan Jinqiao, China	ZB-2301	1:5000	
Peroxidase-Conjugated Goat anti-Mouse IgG(H+L)	Zhongshan Jinqiao, China	ZB-2305	1:5000	
Goat Anti-Mouse IgG (H&L) CY3	Boster Biological Technology, China	BA-1031		1:200
Goat Anti-Rabbit IgG (H&L) FITC	Boster Biological Technology, China	BA-1105		1:200

one-way ANOVA and Fisher's LSD test. $P<0.05$ was considered significant.

Results

Effect of CSE-derived H$_2$S on the colonic mucosa in the DSS-induced ulcerative colitis animal model

All control mice did not die in the experimental modeling process, and the DSS modeling mortality of CSE knockout mice was higher than that of normal mice. However, the mortality of DSS modeling mice was significantly decreased after NaHS treatment (Figure 1A). The body weight of mice in the control group increased steadily with the days. Subsequently, after seven days of modeling with 3% DSS, compared with the control group, the body weight and colon length of mice in the model group decreased and DAI score increased significantly (Figures 1 B–E). Compared with normal mice, CSE knockout mice presented weight loss, shorter colon length, and higher DAI scores ($p<0.01$). NaHS treatment for seven days reduced weight loss, colon length decreases, and DAI scores in both the regular and CSE knockout groups ($p<0.01$). These results suggest that CSE-derived H$_2$S ameliorates DSS-induced damage in mice with ulcerative colitis.

HE staining was used to detect the pathological changes of colonic mucosa in mice with ulcerative colitis induced by DSS. The results show that the epithelial cells and crypt structure are intact, and goblet cells are intact in all the control groups. All DSS model groups had severe lesions, including loss of colonic epithelial cells, distorted crypt structure, and massive inflammatory cell infiltration. However, the damage was more severe in the CSE knockout model group than in the normal

model group (Figure 2, $p<0.01$). Furthermore, compared with the DSS model group, the colon of NaHS-treated mice showed ameliorating colon injury, less inflammatory cell infiltration, and only slight crypt deformation. In addition, the histological damage score caused by DSS was significantly reduced in all NaHS treatment groups (Figure 2, $p<0.01$). Our results suggest that CSE-derived H$_2$S significantly protects colon and attenuates DSS-induced histopathological lesions.

To further investigate the effect of CSE-derived H$_2$S on colon inflammation and injury, immunofluorescence (IF) staining was used to detect the loss of neuronal nucleus (NeuN) and the reduction of myelin basic protein (MBP). As shown in Figure 3, the fluorescence intensity of MBP and NeuN decreased after DSS modeling (compared with the control group, $p<0.01$), suggesting that colitis induced neuron loss and myelin sheath injury of oligodendrocytes. Furthermore, neurons and myelin sheath loss were more severe in CSE KO mice than in WT mice, and NaHS blocked this damage. These results further confirm the protective effect of CSE-derived H$_2$S on neuronal injury in colon.

CSE-derived H$_2$S has a protective effect on the proliferation of EGCs

As shown in Figure 4, the fluorescence intensity of GFAP decreased in colonic mucosa of mice after colitis (compared with the control group; $p< 0.01$). However, the fluorescence intensity of GFAP in colonic mucosa of CSE knockout mice induced by colitis was significantly decreased compared with that of WT mice. In the NaHS treatment, colitis-induced GFAP fluorescence intensity was enhanced considerably. These data suggest that H$_2$S has a significant protective effect on the proliferation of astrocytes.
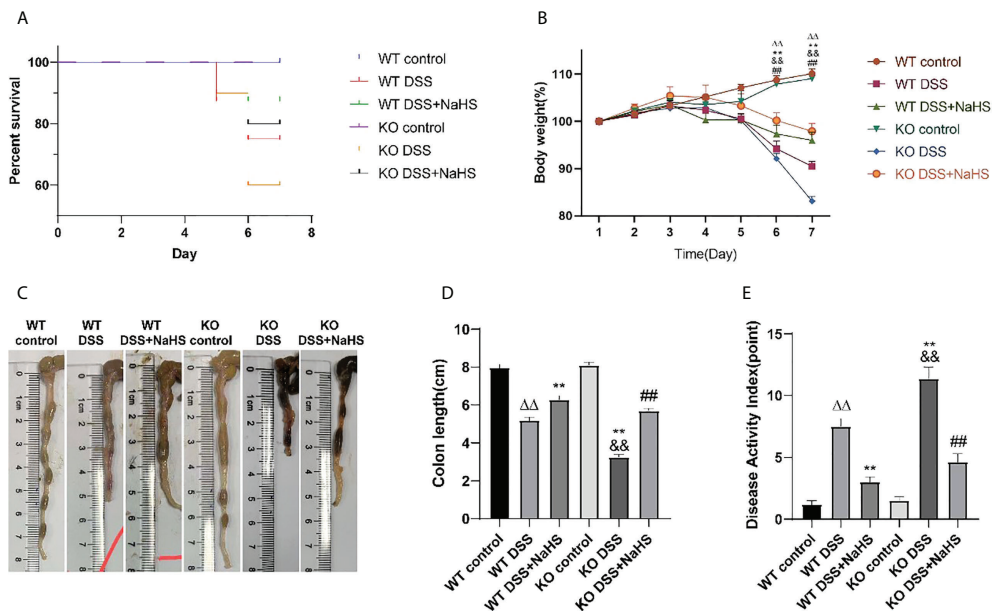
FIGURE 1
Effect of cystathionine-γ-lyase (CSE)-derived hydrogen sulfide (H2S) on dextran sodium sulfate (DSS)-induced ulcerative colitis in mice.
(A) Percent survival. **(B)** Body weight (shown as the percentage of initial body weight). **(C)** Typical pictures of colon. **(D)** Colon length. **(E)** Disease activity index (DAI) score. All data are expressed as the mean $\pm$ SEM, N=6. $\Delta\Delta P\ 0.01$ vs wild-type(WT) control group; **$P < 0.01$ vs WT DSS group; $^{\&\&}P < 0.01$ vs knockout (KO) control group; $^{\#\#}P < 0.01$ vs KO DSS group.
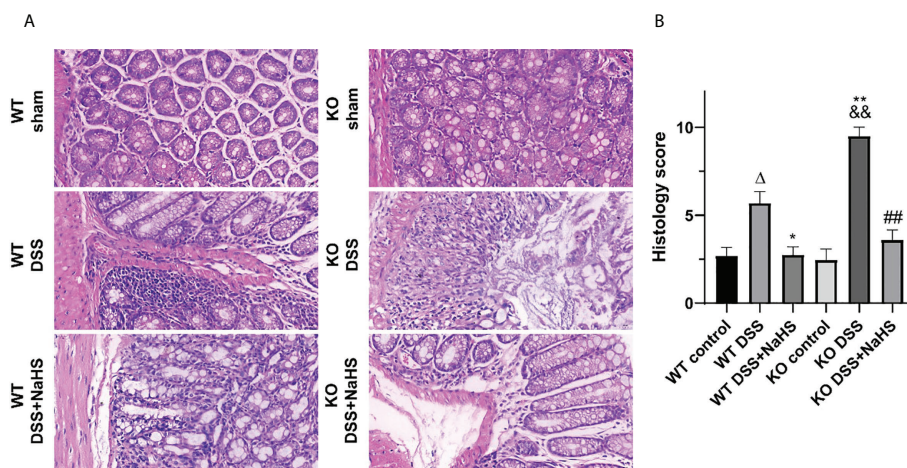
FIGURE 2
Effect of cystathionine-γ-lyase (CSE)-derived hydrogen sulfide (H2S) on colonic injury and histological score (hematoxylin and eosin (H&E) staining). Data are expressed as the mean $\pm$ SEM, N=3. Scale bar = 20μm. **(A)** Typical histological sections stained with H&E (400×magnification). **(B)** Histological scores of colon. $\Delta P < 0.05$ vs wild-type(WT) control group; *$P < 0.05$, **$P < 0.01$ vs WT dextran sodium sulfate (DSS) group; $^{\&\&}P < 0.01$ vs knockout (KO) control group; $^{\#\#}P<0.01$ vs KO DSS group.
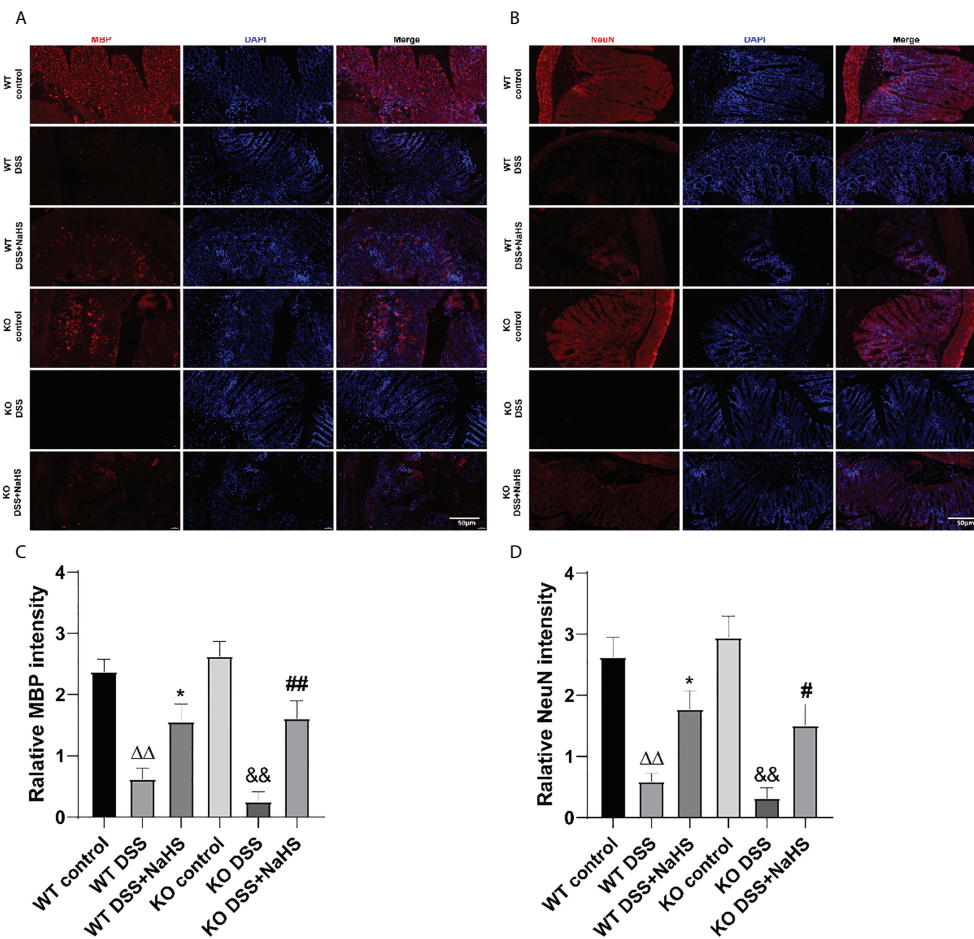
FIGURE 3
Effect of cystathionine-γ-lyase (CSE)-produced hydrogen sulfide (H2S) on the recovery of myelin sheaths and loss of neurons in colon of mice after dextran sodium sulfate (DSS). Scale bar=50μm. **(A)** Myelin basic protein (MBP)-positive cells are red, 4',6-diamidino-2-phenylindole (DAPI) nuclear staining is blue (200×magnification). **(B)** Neuronal Nuclei (NeuN)-positive cells are red, DAPI nuclear staining is blue (200×magnification). **(C)** Relative MBP intensity in the colon of mice. **(D)** Relative NeuN intensity in the colon of mice. *ΔΔP < 0.01 vs wild-type (WT) control group; *P < 0.05 vs WT dextran sodium sulfate (DSS) group; &&P < 0.01 vs knockout (KO) control group; #P<0.05,##P<0.01 vs KO DSS group.*

CSE-derived H$_2$S promoted the transformation of EGCs from type "A1" to "A2"

To further study the transformation of A1/A2 reactive astrocytes in DSS mouse colon, C3 and S100A10 staining were performed. As shown in Figure 5, the fluorescence intensity of C3 and S100A10 in colon decreased seven days after DSS modeling. Besides, the fluorescence intensity of S100A10 and C3 in colon of CSE KO mice decreased more significantly than that of WT mice. In addition, we found that NaHS could further reduce the DSS-induced C3 fluorescence intensity and promote the increase of S100A10 fluorescence intensity in colon. These results confirm that CSE-derived H$_2$S

can promote the reactive proliferation of astrocytes in colitis-induced colon and promote the transformation of astrocytes from "A1" type to "A2" type.

The effects of CSE-derived H$_2$S on the activities of RhoA, ROCK$_1$, and ROCK$_2$ proteins and the content of H$_2$S in colon, as well as the inflammatory cytokines IL-6 and TNF-α in serum of mice

As shown in Figure 6, RhoA, ROCK$_1$, ROCK$_2$ protein activities, and H$_2$S content in colon were detected by ELISA. Compared with the control group, the protein activities of RhoA,
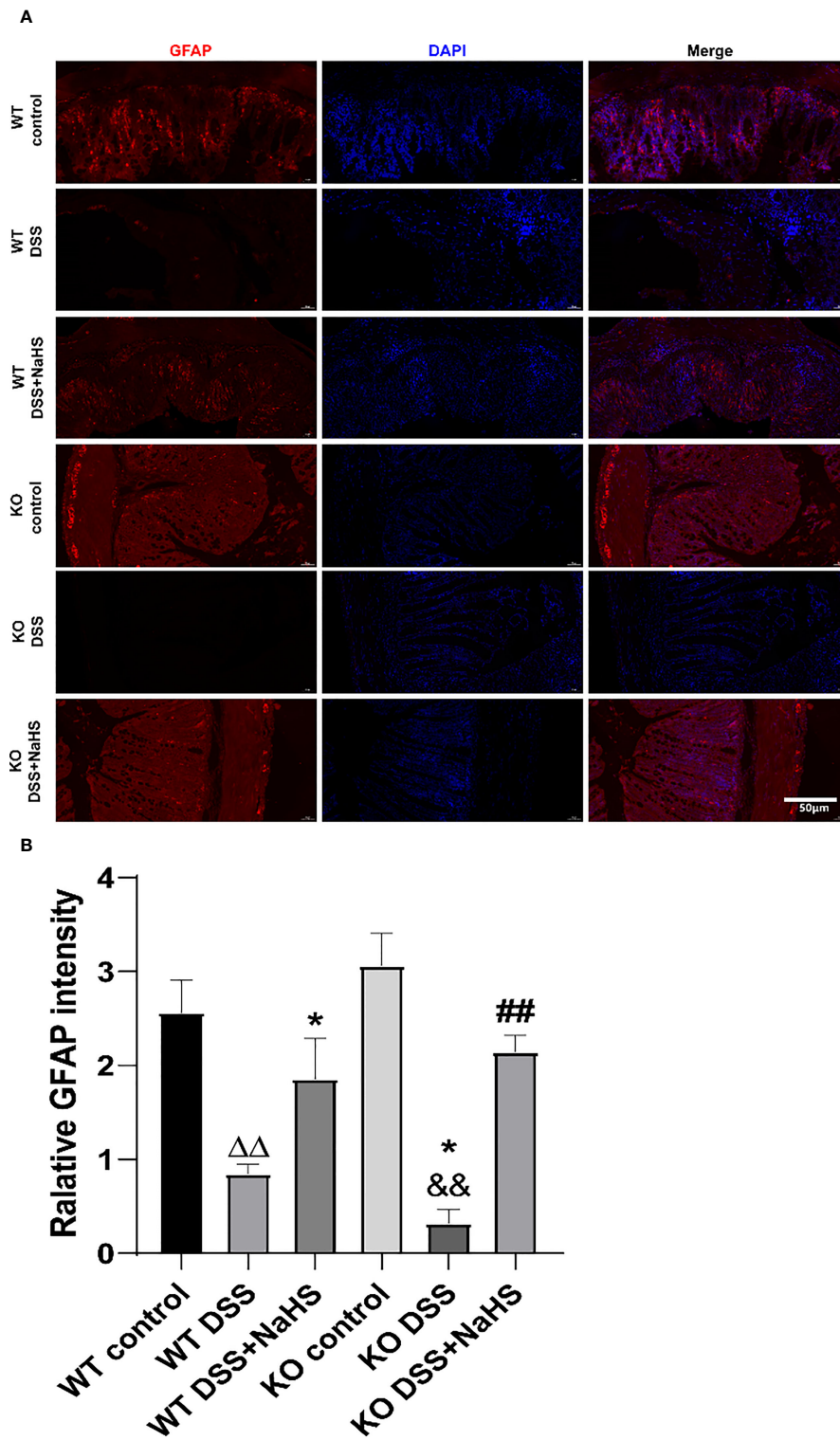
FIGURE 4

Effect of cystathionine-γ-lyase (CSE)-produced hydrogen sulfide (H_2S) on the reactive astrocytes proliferation in colon of mice after dextran sodium sulfate (DSS) (mean$\pm$SEM, N=3). Scale bar=50µm. **(A)** glial fibrillary acidic protein (GFAP)-positive cells are red, 4',6-diamidino-2-phenylindole (DAPI) nuclear staining is blue (200×magnification). **(B)** Relative GFAP intensity in the colon of mice.$^{\Delta\Delta}P < 0.01$ vs wild-type(WT) control group; *P < 0.05 vs WT DSS group; $^{\&\&}P < 0.01$ vs knockout(KO) control group; $^{\#\#}P<0.01$ vs KO DSS group.
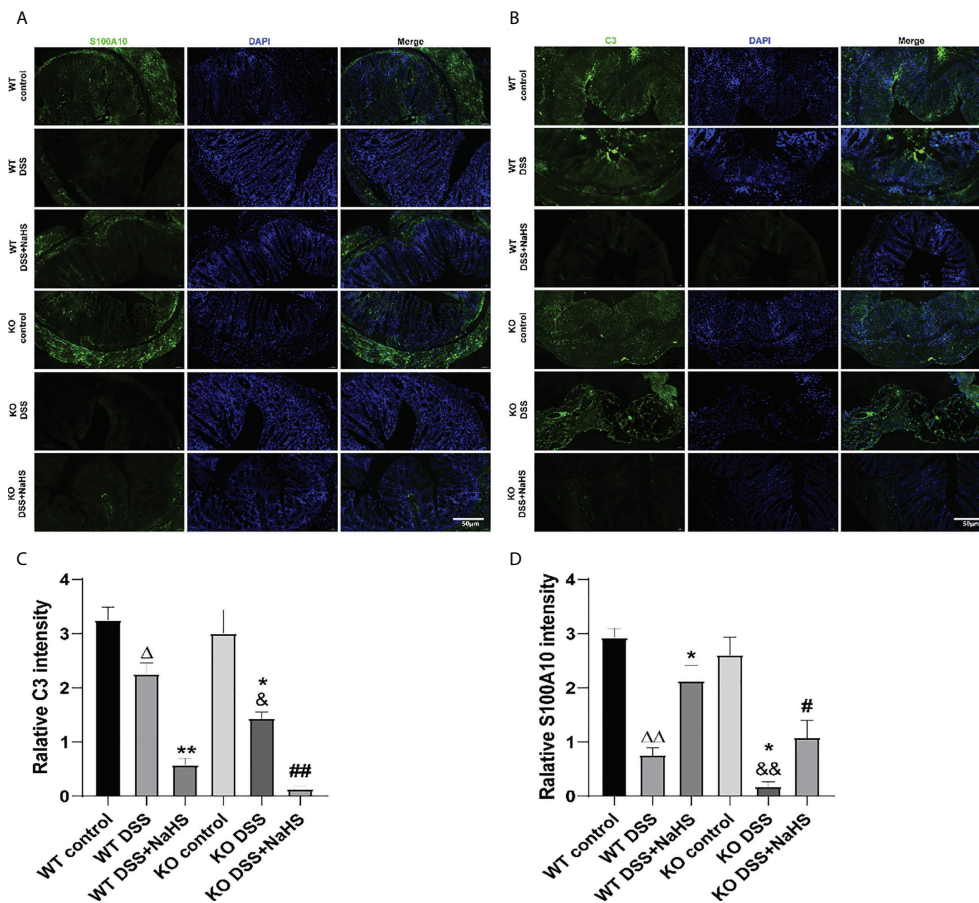
FIGURE 5
Effect of cystathionine-γ-lyase (CSE)-produced hydrogen sulfide (H_2S) on the transformation of enteric glial cells (EGCs) from "A1" to "A2" in colon of mice after dextran sodium sulfate (DSS) (mean $\pm$ SEM, N=3). Scale bar=50μm. **(A)** S100A10-positive cells are green, 4',6-diamidino-2-phenylindole (DAPI) nuclear staining is blue (200×magnification). **(B)** C3-positive cells are green, DAPI nuclear staining is blue (200×magnification). **(C)** Relative S100A10 intensity in the colon of mice. **(D)** Relative C3 intensity in the colon of mice. $^{\Delta}P < 0.05$, $^{\Delta\Delta}P < 0.01$ vs wild-type(WT) control group; $^{*}P < 0.05$, $^{**}P < 0.01$ vs WT DSS group; $^{\&}P < 0.05$, $^{\&\&}P < 0.01$ vs knockout(KO) control group; $^{\#}P<0.05$,$^{\#\#}P<0.01$ vs KO DSS group.

$ROCK_1$ and $ROCK_2$ were enhanced, and the content of H_2S was decreased in the DSS model group. The enhanced RhoA, $ROCK_1$, and $ROCK_2$ protein activities and the reduced H_2S content in the CSE knockout model group were significantly more substantial than those in the normal model group (Figures 6 A–C, F, p< 0.01). In addition, the NaHS treatment group reduced RhoA, $ROCK_1$, and $ROCK_2$ protein activities and significantly enhanced H_2S content in the model group (Figures 6 A–C, F, p< 0.01). The inflammatory cytokines IL-6 and TNF-α in the serum of mice showed the same upregulation trend as the RhoA/ROCK signaling pathway (Figures 6 D, E, p< 0.01). Our results suggest that CSE-derived H_2S protects colon and attenuates inflammatory cytokines IL-6 and TNF-α levels by decreasing RhoA, $ROCK_1$, and $ROCK_2$ protein activities and increasing H_2S.

Effect of CSE-derived H_2S on the expression of RhoA, $ROCK_1$, and $ROCK_2$ proteins in colon

To clarify the correlation between CSE-derived H_2S and RhoA/ROCK pathway, Western blot was used to detect the expression of the RhoA/ROCK pathway. The terms RhoA, $ROCK_1$, and $ROCK_2$ detected by Western blot are shown in Figure 7. The expression of RhoA, $ROCK_1$ and $ROCK_2$ was significantly increased in colitis. Therefore, it is not surprising that colitis-induced RhoA, $ROCK_1$, and $ROCK_2$ expression levels were even higher in CSE KO mice than in WT mice. However, continuous treatment with NaHS from day one after colitis decreased the expression of RhoA, $ROCK_1$, and $ROCK_2$ proteins in CSE KO and WT mice. These data suggest that
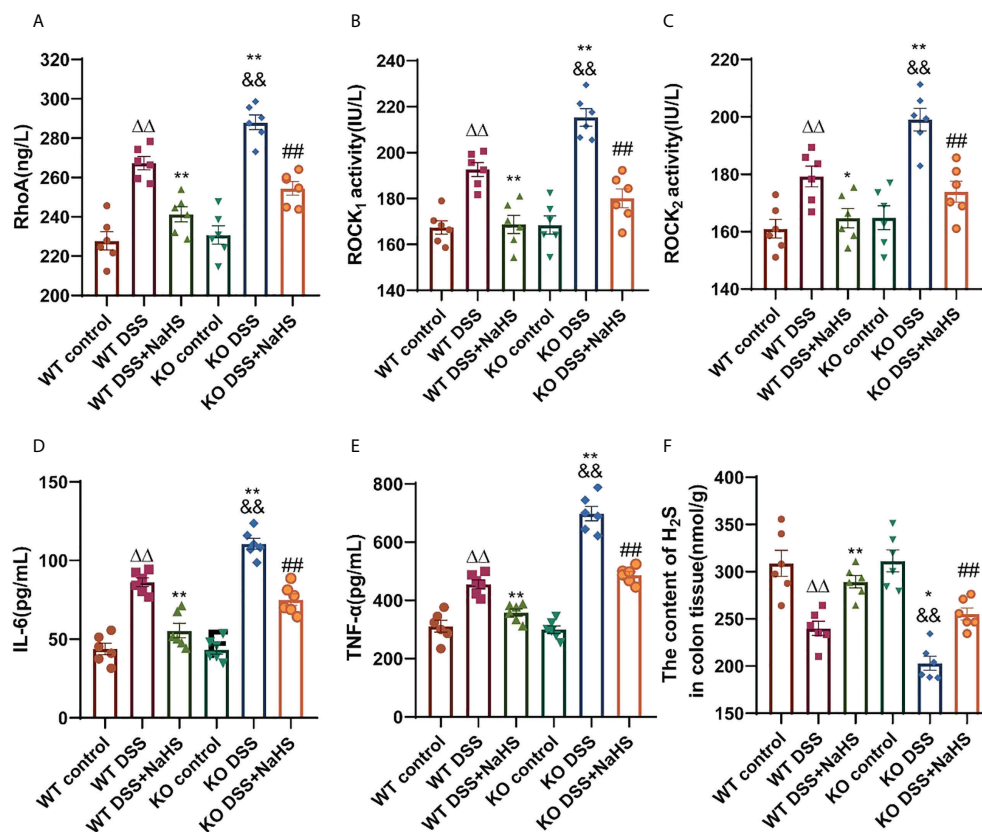
FIGURE 6

Effect of cystathionine-γ-lyase (CSE)-derived hydrogen sulfide (H_2S) on colonic RhoA, Rho kinase 1 ($ROCK_1$), Rho kinase 2 ($ROCK_2$) protein activity and changes of interleukin-6 (IL-6) and tumor necrosis factor-α (TNF-α) in mice sera, and hydrogen sulfide (H_2S) content in colon. Data are expressed as the mean ± SEM, N=6. RhoA activity **(A)**, $ROCK_1$ activity **(B)**, $ROCK_2$ activity **(C)**, IL-6 **(D)**, and TNF-α **(E)** in sera determined by ELISA. The concent of H_2S in colon (nmol/g protein) determined by ELISA **(F)**. $^{\Delta\Delta}P < 0.01$ vs wild-type(WT) control group; $^*P < 0.05$, $^{**}P < 0.01$ vs WT dextran sodium sulfate (DSS) group; $^{\&\&}P < 0.01$ vs knockout (KO) control group; $^{\#\#}P<0.01$ vs KO DSS group.

CSE-derived H_2S inhibits the activation of the RhoA/ROCK pathway.

Effect of CSE-derived H_2S on the expression of GFAP, C3, and S100A10 proteins in colon

We attempted to test the expression of GFAP, A1 astrocyte labeled C3 protein, and A2 astrocyte labeled S100A10 protein in the colon by Western blot to investigate whether H_2S produced by CSE affected the proliferation of reactive astrocytes containing A1 and A2 types. The results in Figure 8 indicate that GFAP expression and C3 protein and S100A10 expression are decreased in the colonic mucosa of mice after colitis. In addition, colitis-induced decreases in GFAP, C3 protein, and S100A10 expression were more significant in CSE KO mice than in WT mice. However, in WT and CSE KO mice, there were no significant differences in GFAP, C3, and S100A10 protein

expression, indicating that CSE KO had no effect on GFAP, C3, and S100A10 protein expression. Still, colitis exacerbated the decrease of GFAP, C3, and S100A10 protein expression. In addition, as shown in the figure, NaHS inhibits the decreased expression of GFAP and S100A10 but further inhibits the expression of C3, suggesting that H_2S produced by CSE inhibits the proliferation of reactive astrocytes of the type A1, but enhances the proliferation of type A2 astrocytes in mouse colon after induction colitis.

Discussion

In the present study, the DSS-induced colitis was ameliorated by the H_2S donor NaHS, which was manifested by improved clinical parameters and decreased serum levels of IL-6 and TNF-α. More severe changes in IL-6 and TNF-α, and reduced H_2S content in colon were observed in CSE knockout mice. Macrophages in the colon will trigger and exacerbate DSS-
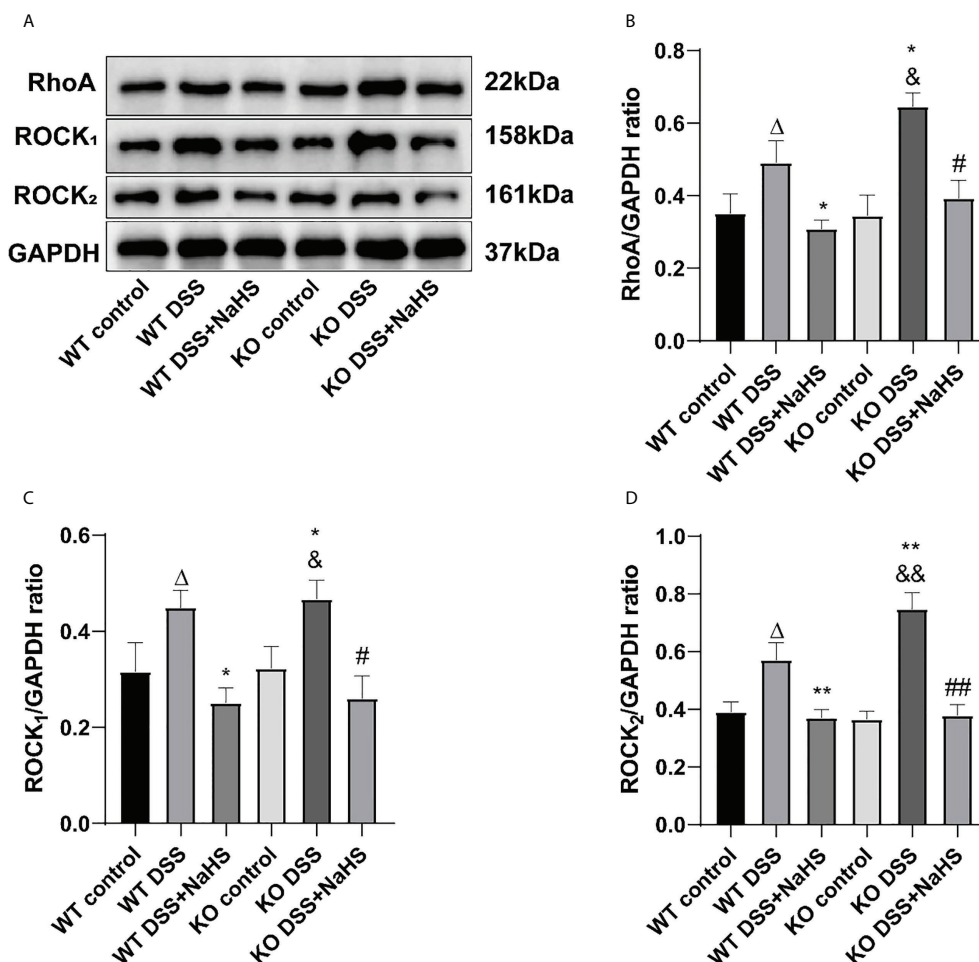
FIGURE 7

Effects of cystathionine-γ-lyase (CSE)-derived hydrogen sulfide (H_2S) on the expression of RhoA, Rho kinase 1 ($ROCK_1$), and Rho kinase 2 ($ROCK_2$) proteins in colon. Data are expressed as the mean $\pm$ SEM, N=3. **(A)** The bands of RhoA, $ROCK_1$, and $ROCK_2$. **(B)** The relative expression of RhoA in colon. **(C)** The relative expression of $ROCK_1$ in colon. **(D)** The relative expression of $ROCK_2$ in colon. $^{\Delta}P < 0.05$ vs wild-type(WT) control group; $^*P < 0.05$, $^{**}P < 0.01$ vs WT dextran sodium sulfate (DSS) group; $^{\&}P < 0.05$, $^{\&\&}P < 0.01$ vs knockout (KO) control group; $^{\#}P<0.05$, $^{\#\#}P<0.01$ vs KO DSS group.

induced colitis by releasing cytokines, such as IL-6, TNF-α, and IL-1β ([20]). It has been reported that H_2S has an anti-inflammatory effect, which may inhibit chromatin openness at the IL-6 and TNF-α promoters by suppressing histone acetylation ([21], [22]). NaHS can only partially ameliorate the more malignant colitis in CSE knockout mice, which indicates that CSE-derived endogenous H_2S plays a crucial protective effect against DSS-induced colitis.

H_2S is produced throughout the gastrointestinal tract and helps maintain mucosal integrity ([23]). H_2S may have pro-inflammatory or anti-inflammatory effects depending on the dosage and route of administration ([24]). Subcutaneous injection of low-dose NaHS (~5.6mg/kg) showed an anti-inflammatory effect in the C57BL6/J sepsis model induced by cecal ligation and

puncture (CLP) ([25]). However, Zhang et al. found the pro-inflammatory effect of H_2S donor NaHS (10mg/kg i.p.) on CLP-induced sepsis and an inhibitor of CSE [DL-propargylglycine (PAG; 50 mg/kg i.p.)], which could reverse this effect ([26]). DSS-induced colitis in mice mimics clinical symptoms and histopathological features in human UC, with weight loss, diarrhea, and occult blood in stools ([27]). In this study, more serious clinical manifestations such as DAI scores, colon length, weight loss, fecal occult blood, and histopathological features of colon were observed in CSE knockout mice. Exogenous H_2S can relieve signs and symptoms of DSS-induced UC, with reduced disease activity index (DAI) scores, improved colon length shortening, improved histopathological inflammation, and reduced body weight loss ([16], [28], [29]). However, the effect and
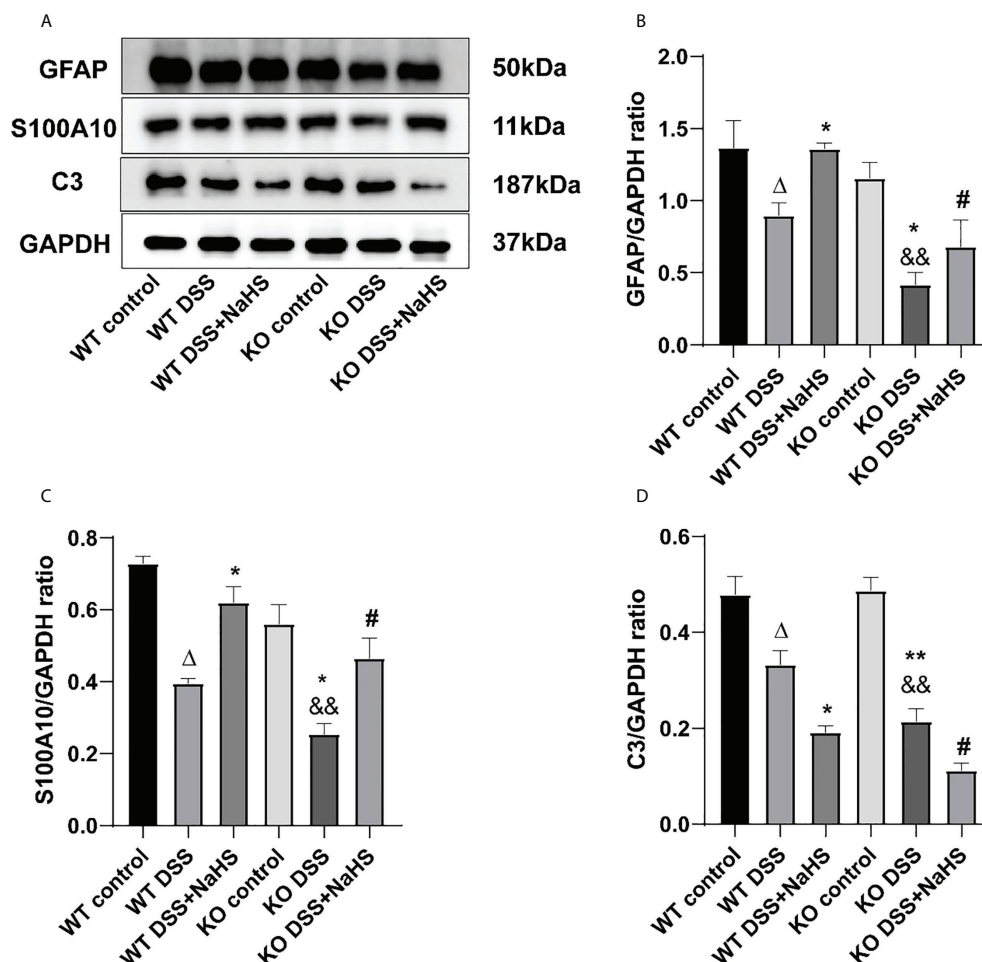
FIGURE 8

Effects of cystathionine-γ-lyase (CSE)-derived hydrogen sulfide (H2S) on the expression of glial fibrillary acidic protein (GFAP), S100A10, and C3 proteins in colon. Data are expressed as the mean $\pm$ SEM, N=3. **(A)** The bands of GFAP, S100A10, and C3. **(B)** The relative expression of GFAP in colon. **(C)** The relative expression of S100A10 in colon. **(D)** The relative expression of C3 in colon. $^{\Delta}P < 0.05$ vs wild-type (WT) control group; $^{*}P < 0.05$, $^{**}P < 0.01$ vs WT dextran sodium sulfate (DSS) group; $^{\&\&}P < 0.01$ vs knockout (KO) control group; $^{\#}P < 0.05$ vs KO DSS group.

mechanism of endogenous H_2S on colitis remain unclear. CSE/H_2S regulates circadian-clock genes and maintains cellular glutathione biosynthesis and glucose homeostasis in C2C12 myotubes (30, 31). In the present study, CSE knockout mice were more susceptible to DSS-induced colitis than wild-type mice, which was consistent with the previous report, indicating that CSE-derived endogenous H_2S plays a crucial protective effect against DSS-induced colitis (32).

Our findings show that RhoA/ROCK signal pathway is upregulated in colitis mice. Not surprisingly, the upregulation of the RhoA/ROCK pathway is more remarkable in CSE KO mice. NaHS serves as an effective UC treatment *via* inhibiting RhoA/ROCK signal pathway. The RhoA/ROCK (Rho-kinase) signaling pathway has been demonstrated to play an essential role in regulating biological pathways, such as those that impact smooth muscle tension levels and different kinds of physiological characteristics associated with actin cytoskeletal changes, including migration, cell adhesion, contraction, and motility (33). RhoA/ROCK$_1$ dependent actomyosin contractility was increased due to cortactin deficiency, a critical regulator of intestinal epithelial barrier functions, causing altered molecular composition of epithelial junctions and increased intestinal epithelial permeability (34). H_2S protects the central nervous system (CNS) by acting as an antioxidant and regulates cell signaling (35). It has been reported that CSE-derived H_2S could inhibit the reactive proliferation of astrocytes and promote the recovery of neural functional deficits in mice induced by cerebral I/R injury *via* inhibition of the RhoA/ROCK$_2$ signal pathway

(17). However, it remains unclear whether CSE-derived H_2S can play a similar role in the DSS-induced colitis model. In the present study, our findings indicate that CSE-derived H_2S can promote the recovery of mice gut functional deficits from DSS-induced colitis *via* inhibition of the RhoA/ROCK signal pathway.

The enteric nervous system consists of neurons and EGCs. Compelling evidence demonstrated that enteric glia played a central role in regulating homeostasis in the enteric nervous system (36, 37). Active signaling mechanisms between enteric glia and neurons modulate gastrointestinal reflexes. In certain circumstances, its function drives the neuroinflammatory process leading to long-term dysfunction. Bidirectional communication between enteric glia and immune cells contributes to gastrointestinal immune homeostasis (36). The present study was designed to deeply elucidate the pathological changes of intestinal nerve cells in UC and determine whether the effects of endogenous H_2S on alleviating UC were associated with improved functional defects of EGCs. Although enteric glial cells are extensive heterogeneity and phenotypic plasticity, the majority of glia in the myenteric plexus are GFAP positive (38). GFAP gene and protein expression have been a useful marker for assessing astrocyte reactivity in animal injury and disease models and in human pathological specimens (39). Our findings show that GFAP expression indicative of reactive glia is reduced in the DSS-induced colitis mice and worse in the CSE knockout mice. NaHS significantly increased GFAP protein levels during inflammation, and we observed corresponding changes in the GFAP Immunofluorescence assay. CSE-derived endogenous H_2S had a significant effect on preventing the reactiveness of glial processes during colitis.

Enteric glia secretes neuroprotective compounds and possesses neuroprotective properties (40). Intestinal inflammation is associated with the leukocyte infiltration into or surrounding the neuronal ganglia of the enteric nervous system (ENS), which is termed plexitis or ganglionitis (41). In this study, the staining results of NeuN and MBP in the colon indicate DSS-induced neuron damage and myelin loss of glial cells in the mice colitis model. NeuN is a neuronal-specific nuclear protein that serves as an excellent marker for neurons in the central and peripheral nervous systems of vertebrate embryos and adults (42). Nassauw et al. reported that the cytoplasmic expression of NeuN is an exclusive marker of intrinsic primary afferent neurons (IPANs) in the gut (43). MBP is a membrane actin-binding protein that participates in the transmission of extracellular signals to the cytoskeleton in oligodendrocytes and tight junctions in myelin (44). Our results showed that CSE-derived endogenous H_2S had an effect on protecting the intestinal neurons and glial cells during colitis.

In this study, we found that C3 and S100A10 protein expression were reduced in colon of DSS-induced colitis mice, which were lower in that of CSE knockout mice. NaHS treatment markedly blocked the decrease of S100A10 expression, but further reduced C3 expression. The same results were confirmed by immunofluorescence assay. Neuroinflammation and ischemia-induced two different phenotypes of reactive astrocytes, which are termed A1 and A2, in analogy to the M1/M2 macrophage nomenclature (39, 45). The upregulation of H_2S levels can have beneficial effects on glucose homeostasis through activation of PGC-1α/FNDC5/irisin signaling pathway (46). The anti-inflammatory mechanism of irisin includes reducing macrophage proliferation and inducing alternating activation (M2 type) macrophage polarization (47). Recent studies demonstrated that different initiating CNS injuries could elicit two types of "reactive" astrocytes with different properties, type A1 is harmful and type A2 is beneficial or with reparative functions (39). Complement component C3 is one of the most characteristic and highly upregulated genes in A1s but is not expressed in A2 reactive astrocytes, while S100A10 is specifically expressed in the A2 type astrocytes (45, 48). To our knowledge, the heterogeneity of reactive astrocytes in the gut has not been reported and requires further study. Our previous study showed that the number of astrocytes in the DSS-induced colitis colon was decreased and H_2S had an inhibitory effect on the decrease and promoted the transformation of the A1 type into the A2 type (16). The present results indicate that CSE-derived endogenous H_2S plays an important role in protecting colitis by promoting the proliferation of EGCs, suppressing the A1 phenotype conversion in astrocytes and promoting the transformation of astrocytes from "A1" type to "A2" type. These findings suggest that preserving the loss of EGCs or transforming the pathologic astrocytes into useful ones can reverse ENS dysfunction.

In conclusion, these findings indicate that CSE-derived H_2S can preserve the function of EGCs *via* inhibiting the reactive proliferation and promote EGCs transformation, and inhibition of the RhoA/ROCK signal pathway in mice model of colitis induced by DSS.

Data availability statement

The raw data supporting the conclusions of this article will be made available by the authors, without undue reservation.

Ethics statement

The animal study was reviewed and approved by Animal Experimental Ethics Review Committee of the University of Science and Technology of China.

Author contributions

SW and WJ conceived the ideas and designed the study. SW and YD performed laboratory work. All authors analyzed data. SW and WJ wrote the paper and the manuscript was reviewed and commented on by all authors. All authors contributed to the article and approved the submitted version.

Acknowledgments

We are grateful to Dr. Xudong Yuan and Dr. Yiyao Tu for the colon pathological analysis.

Conflict of interest

The authors declare that the research was conducted in the absence of any commercial or financial relationships that could be construed as a potential conflict of interest.

Publisher's note

All claims expressed in this article are solely those of the authors and do not necessarily represent those of their affiliated organizations, or those of the publisher, the editors and the reviewers. Any product that may be evaluated in this article, or claim that may be made by its manufacturer, is not guaranteed or endorsed by the publisher.

References

1. Mak WY, Zhao M, Ng SC, Burisch J. The epidemiology of inflammatory bowel disease: East meets west. *J Gastroenterol Hepatol* (2020) 35:380–9. doi: 10.1111/jgh.14872

2. Qiu Y, Ren W, Liu Y, Chen WE, Pan XH, Ren JJ. Disease burden of inflammatory bowel disease in China from 1990 to 2017: Findings from the global burden of diseases 2017. *EClinicalMedicine* (2020) 27:100544. doi: 10.1016/j.eclinm.2020.100544

3. Kobayashi T, Siegmund B, Le Berre C, Wei SC, Ferrante M, Shen B, et al. Ulcerative colitis. *Nat Rev Dis Primers* (2020) 6:74. doi: 10.1038/s41572-020-0205-x

4. Li H, Fan C, Lu H, Feng C, He P, Yang X, et al. Protective role of berberine on ulcerative colitis through modulating enteric glial cells-intestinal epithelial cells-immune cells interactions. *Acta Pharm Sinica. B* (2020) 10:447–61. doi: 10.1016/j.apsb.2019.08.006

5. Boesmans W, Nash A, Tasnády KR, Yang W, Stamp LA, Hao MM. Development, diversity, and neurogenic capacity of enteric glia. *Front Cell Dev Biol* (2021) 9:775102. doi: 10.3389/fcell.2021.775102

6. Bush TG, Savidge TC, Freeman TC, Cox HJ, Campbell EA, Mucke L, et al. Fulminant jejuno-ileitis following ablation of enteric glia in adult transgenic mice. *Cell* (1998) 93:189–201. doi: 10.1016/s0092-8674(00)81571-8

7. Shajib MS, Baranov A, Khan WI. Diverse effects of gut-derived serotonin in intestinal inflammation. *ACS Chem Neurosci* (2017) 8:920–31. doi: 10.1021/acschemneuro.6b00414

8. Walldorf J, Porzner M, Neumann M, Joodi G, Niess JH, von Boyen G, et al. The selective 5-HT1A agonist SR57746A protects intestinal epithelial cells and enteric glia cells and promotes mucosal recovery in experimental colitis. *Inflammatory bowel Dis* (2021) 28(3):423–33. doi: 10.1093/ibd/izab191

9. Singh SB, Lin HC. Hydrogen sulfide in physiology and diseases of the digestive tract. *Microorganisms* (2015) 3(4):866–89. doi: 10.3390/microorganisms3040866

10. Gil V, Gallego D, Jiménez M. Effects of inhibitors of hydrogen sulphide synthesis on rat colonic motility. *Br J Pharmacol* (2011) 164:485–98. doi: 10.1111/j.1476-5381.2011.01431.x

11. Grasa L, Abecia L, Peña-Cearra A, Robles S, Layunta E, Latorre E, et al. TLR2 and TLR4 interact with sulfide system in the modulation of mouse colonic motility. *Neurogastroenterol Motil Off J Eur Gastrointestinal Motil Soc* (2019) 31: e13648. doi: 10.1111/nmo.13648

12. Paul BD, Snyder SH. H2S signalling through protein sulfhydration and beyond. *Nat Rev Mol Cell Biol* (2012) 13:499–507. doi: 10.1038/nrm3391

13. Segain JP, Raingeard de la Blétière D, Sauzeau V, Bourreille A, Hilaret G, Cario-Toumaniantz C, et al. Rho kinase blockade prevents inflammation *via* nuclear factor kappa b inhibition: evidence in crohn's disease and experimental colitis. *Gastroenterology* (2003) 124:1180–7. doi: 10.1016/s0016-5085(03)00283-x

14. Fang K, Law I, Padua D, Sideri A, Huang V, Kevil CG, et al. MicroRNA-31-3p is involved in substance p (SP)-associated inflammation in human colonic epithelial cells and experimental colitis. *Am J Pathol* (2018) 188:586–99. doi: 10.1016/j.ajpath.2017.10.023

15. Wang Y, Shou Z, Fan H, Xu M, Chen Q, Tang Q, et al. Protective effects of oxymatrine against DSS-induced acute intestinal inflammation in mice *via* blocking the RhoA/ROCK signaling pathway. *Bioscience Rep* (2019) 39(7): BSR20182297. doi: 10.1042/BSR20182297

16. Ding Y, Liu B, Zhang Y, Fang F, Li X, Wang S, et al. Hydrogen sulphide protects mice against the mutual aggravation of cerebral ischaemia/reperfusion injury and colitis. *Eur J Pharmacol* (2021) 914:174682. doi: 10.1016/j.ejphar.2021.174682

17. Zhang Y, Li K, Wang X, Ding Y, Ren Z, Fang J, et al. CSE-Derived H2S inhibits reactive astrocytes proliferation and promotes neural functional recovery after cerebral Ischemia/Reperfusion injury in mice *Via* inhibition of RhoA/ROCK2 pathway. *ACS Chem Neurosci* (2021) 12:2580–90. doi: 10.1021/acschemneuro.0c00674

18. Wirtz S, Popp V, Kindermann M, Gerlach K, Weigmann B, Fichtner-Feigl, et al. Chemically induced mouse models of acute and chronic intestinal inflammation. *Nat Protoc* (2017) 12(7):1295–309. doi: 10.1038/nprot.2017.044

19. Szabady RL, Louissaint C, Lubben A, Xie B, Reeksting S, Tuohy C, et al. Intestinal p-glycoprotein exports endocannabinoids to prevent inflammation and maintain homeostasis. *J Clin Invest* (2018) 128(9):4044–56. doi: 10.1172/JCI96817

20. Zaki MH, Lamkanfi M, Kanneganti TD. The Nlrp3 inflammasome: Contributions to intestinal homeostasis. *Trends Immunol* (2011) 32:171–9. doi: 10.1016/j.it.2011.02.002

21. Wallace JL, Wang R. Hydrogen sulfide-based therapeutics: exploiting a unique but ubiquitous gasotransmitter. *Nat Rev Drug Discovery* (2015) 14:329–45. doi: 10.1038/nrd4433

22. Rios EC, Szczesny B, Soriano FG, Olah G, Szabo C. Hydrogen sulfide attenuates cytokine production through the modulation of chromatin remodeling. *Int J Mol Med* (2015) 35(6):1741–6. doi: 10.3892/ijmm.2015.2176

23. Gemici B, Wallace JL. Anti-inflammatory and cytoprotective properties of hydrogen sulfide. *Methods Enzymol* (2015) 555:169–93. doi: 10.1016/bs.mie.2014.11.034

24. Suzuki Y, Saito J, Munakata M, Shibata Y. Hydrogen sulfide as a novel biomarker of asthma and chronic obstructive pulmonary disease. *Allergol Int* (2021) 70(2):181–9. doi: 10.1016/j.alit.2020.10.003

25. Ferlito M, Wang Q, Fulton WB, Colombani PM, Marchionni L, Fox-Talbot K, et al. Hydrogen sulfide [corrected] increases survival during sepsis: Protective effect of CHOP inhibition. *J Immunol* (2014) 192(4):1806–14. doi: 10.4049/jimmunol.1300835

26. Zhang H, Zhi L, Moore PK, Bhatia M. Role of hydrogen sulfide in cecal ligation and puncture-induced sepsis in the mouse. *Am J Physiol Lung Cell Mol Physiol* (2006) 290(6):L1193–1201. doi: 10.1152/ajplung.00489.2005

27. Chassaing B, Aitken JD, Malleshappa M, Vijay-Kumar M. Dextran sulfate sodium (DSS)-induced colitis in mice. *Curr Protoc Immunol* (2014) 104:15.25.1–15.25.14. doi: 10.1002/0471142735.im1525s104

28. Hirata I, Naito Y, Takagi T, Mizushima K, Suzuki T, Omatsu T, et al. Endogenous hydrogen sulfide is an anti-inflammatory molecule in dextran sodium

sulfate-induced colitis in mice. *Dig Dis Sci* (2011) 56(5):1379–86. doi: 10.1007/s10620-010-1461-5

29. Zhao H, Yan R, Zhou X, Ji F, Zhang B. Hydrogen sulfide improves colonic barrier integrity in DSS-induced inflammation in caco-2 cells and mice. *Int Immunopharmacol* (2016) 39:121–7. doi: 10.1016/j.intimp.2016.07.020

30. Parsanathan R, Jain SK. Hydrogen sulfide increases glutathione biosynthesis, and glucose uptake and utilisation in C(2)C(12) mouse myotubes. *Free Radic Res* (2018) 52(2):288–303. doi: 10.1080/10715762.2018.1431626

31. Parsanathan R, Jain SK. Hydrogen sulfide regulates circadian-clock genes in C(2)C(12) myotubes and the muscle of high-fat-diet-fed mice. *Arch Biochem Biophys* (2019) 672:108054. doi: 10.1016/j.abb.2019.07.019

32. Qin M, Long F, Wu W, Yang D, Huang M, Xiao C, et al. Hydrogen sulfide protects against DSS-induced colitis by inhibiting NLRP3 inflammasome. *Free Radic Biol Med* (2019) 137:99–109. doi: 10.1016/j.freeradbiomed.2019.04.025

33. Al-Shboul O. The role of the RhoA/ROCK pathway in gender-dependent differences in gastric smooth muscle contraction. *J Physiol Sci* (2016) 66:85–92. doi: 10.1007/s12576-015-0400-9

34. Citalán-Madrid AF, Vargas-Robles H, García-Ponce A, Shibayama M, Betanzos A, Nava P, et al. Cortactin deficiency causes increased RhoA/ROCK1-dependent actomyosin contractility, intestinal epithelial barrier dysfunction, and disproportionately severe DSS-induced colitis. *Mucosal Immunol* (2017) 10(5):1237–47. doi: 10.1038/mi.2016.136

35. Shefa U, Kim MS, Jeong NY, Jung J. Antioxidant and cell-signaling functions of hydrogen sulfide in the central nervous system. *Oxid Med Cell Longev* (2018) 2018:1873962. doi: 10.1155/2018/1873962

36. Seguella L, Gulbransen BD. Enteric glial biology, intercellular signalling and roles in gastrointestinal disease. *Nat Rev Gastroenterol Hepatol* (2021) 18:571–87. doi: 10.1038/s41575-021-00423-7

37. Neunlist M, Rolli-Derkinderen M, Latorre R, Van Landeghem L, Coron E, Derkinderen P, et al. Enteric glial cells: Recent developments and future directions. *Gastroenterology* (2014) 147(6):1230–7. doi: 10.1053/j.gastro.2014.09.040

38. Boesmans W, Lasrado R, Vanden Berghe P, Pachnis V. Heterogeneity and phenotypic plasticity of glial cells in the mammalian enteric nervous system. *Glia* (2015) 63(2):229–41. doi: 10.1002/glia.22746

39. Liddelow SA, Barres BA. Reactive astrocytes: Production, function, and therapeutic potential. *Immunity* (2017) 46:957–67. doi: 10.1016/j.immuni.2017.06.006

40. Abdo H, Derkinderen P, Gomes P, Chevalier J, Aubert P, Masson D, et al. Enteric glial cells protect neurons from oxidative stress in part *via* reduced glutathione. *FASEB J* (2010) 24(5):1082–94. doi: 10.1096/fj.09-139519

41. Stavely R, Abalo R, Nurgali K. Targeting enteric neurons and plexitis for the management of inflammatory bowel disease. *Curr Drug Targets* (2020) 21:1428–39. doi: 10.2174/1389450121666200516173242

42. Mullen RJ, Buck CR, Smith AM. NeuN, a neuronal specific nuclear protein in vertebrates. *Development* (1992) 116:201–11. doi: 10.1242/dev.116.1.201

43. Van Nassauw L, Wu M, De Jonge F, Adriaensen D, Timmermans JP. Cytoplasmic, but not nuclear, expression of the neuronal nuclei (NeuN) antibody is an exclusive feature of dogiel type II neurons in the guinea-pig gastrointestinal tract. *Histochem Cell Biol* (2005) 124(5):369–77. doi: 10.1007/s00418-005-0019-7

44. Boggs JM. Myelin basic protein: A multifunctional protein. *Cell Mol Life Sci* (2006) 63:1945–61. doi: 10.1007/s00018-006-6094-7

45. Liddelow SA, Guttenplan KA, Clarke LE, Bennett FC, Bohlen CJ, Schirmer L, et al. Neurotoxic reactive astrocytes are induced by activated microglia. *Nature* (2017) 541(7638):481–7. doi: 10.1038/nature21029

46. Parsanathan R, Jain SK. Hydrogen sulfide regulates irisin and glucose metabolism in myotubes and muscle of HFD-fed diabetic mice. *Antioxidants (Basel)* (2022) 11(7):1369. doi: 10.3390/antiox11071369

47. Slate-Romano JJ, Yano N, Zhao TC. Irisin reduces inflammatory signaling pathways in inflammation-mediated metabolic syndrome. *Mol Cell Endocrinol* (2022) 552:111676. doi: 10.1016/j.mce.2022.111676

48. Giovannoni F, Quintana FJ. The role of astrocytes in CNS inflammation. *Trends Immunol* (2020) 41:805–19. doi: 10.1016/j.it.2020.07.007